

Simultaneous analysis of three-dimensional percolation models

Xiao Xu,¹ Junfeng Wang,^{1,2} Jian-Ping Lv,^{3,*} and Youjin Deng^{1,†}

¹*Hefei National Laboratory for Physical Sciences at Microscale and Department of Modern Physics, University of Science and Technology of China, Hefei, Anhui 230026, China*

²*School of Electronic Science and Applied Physics, Hefei University of Technology, Hefei, Anhui 230009, China*

³*Department of Physics, China University of Mining and Technology, Xuzhou 221116, China*

(Dated: March 1, 2018)

We simulate the bond and site percolation models on several three-dimensional lattices, including the diamond, body-centered cubic, and face-centered cubic lattices. As on the simple-cubic lattice [Phys. Rev. E, **87** 052107 (2013)], it is observed that in comparison with dimensionless ratios based on cluster-size distribution, certain wrapping probabilities exhibit weaker finite-size corrections and are more sensitive to the deviation from percolation threshold p_c , and thus provide a powerful means for determining p_c . We analyze the numerical data of the wrapping probabilities simultaneously such that universal parameters are shared by the aforementioned models, and thus significantly improved estimates of p_c are obtained.

PACS numbers: 05.50.+q (lattice theory and statistics), 05.70.Jk (critical point phenomena), 64.60.ah (percolation), 64.60.F- (equilibrium properties near critical points, critical exponents)

Keywords:

I. INTRODUCTION

Percolation is a geometric model which involves the random occupation of sites or edges of a regular lattice, and was first introduced by Broadbent and Hammmersley [1]. As a cornerstone of the theory of critical phenomena [2] and a central topic in probability theory [3, 4], percolation attracts much attention.

The two-dimensional (2D) case has been studied extensively, and several exact results are known. Coulomb gas arguments [5] and conformal field theory [6] predict the exact values of the bulk critical exponents $\beta = 5/36$ and $\nu = 4/3$, which have been confirmed rigorously in the specific case of site percolation on the triangular lattice [7]. Moreover, percolation thresholds p_c on many 2D lattices are exactly known [8], or known to very high precision [9, 10]. For $d > 2$, estimates of p_c have to rely on numerical methods such as series expansions and Monte Carlo simulations, while the critical exponents $\beta = 1$ and $d\nu = 3$ for $d \geq d_c = 6$ can be predicted by mean-field theory [11] and even proved rigorously [12, 13] for $d \geq 19$. A more or less thorough list of percolation thresholds for $d \in [2, 13]$ is summarized on the Wikipedia webpage: http://en.wikipedia.org/wiki/Percolation_threshold.

Very recently, two of the authors and coworkers carried out an extensive simulation of bond and site percolation on the simple-cubic (SC) lattice up to system size $512 \times 512 \times 512$ [14], and determined the percolation thresholds and critical exponents to high precision. It was observed that in comparison with dimensionless ratios based on cluster-size moments, the wrapping proba-

bilities suffer from weaker finite-size corrections and are more sensitive to the deviation $p - p_c$ from the percolation threshold. As an extension of Ref. [14], the present work studies percolation on other common three-dimensional (3D) lattices, and shows that such an observation generally holds in 3D percolation. Meanwhile, with the employment of a simultaneous fitting procedure developed in Ref. [15] and the help of the accurate data reported in Ref. [14], we also provide high-precision estimates of p_c for the site and bond percolation on the diamond (DM), body-centered cubic (BCC), and face-centered cubic (FCC) lattices.

The remainder of this paper is organized as follows. Section II defines the sampled quantities of interest. In Sec. III, the numerical data of the dimensionless ratios and the wrapping probabilities are analyzed separately for each percolation model. Then, a simultaneous fitting of the wrapping probabilities is carried out to determine percolation threshold p_c . Section IV presents the analyses for other quantities at criticality p_c , and a brief discussion is given in Sec. V.

II. SAMPLED QUANTITIES

We study bond and site percolation on three-dimensional lattices including the DM, SC, BCC, and FCC lattices, illustrated in Fig. 1. The simulations follow the standard method: each edge/site is occupied with probability p and clusters are constructed by the breadth-first search.

The sampled quantities are the same as in Ref. [14]. For completeness, they are described in the following.

- The number of occupied bonds \mathcal{N}_b or sites \mathcal{N}_s .
- The number of clusters \mathcal{N}_c .

*Electronic address: phys.lv@gmail.com

†Electronic address: yjdeng@ustc.edu.cn

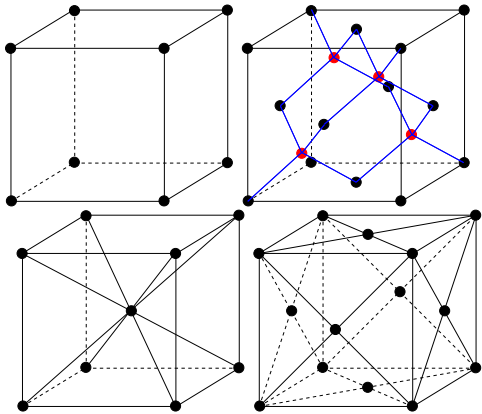


FIG. 1: Three-dimensional lattices: (left-top), SC; (right-top), DM; (left-bottom), BCC; (right-bottom), FCC.

- The largest-cluster size \mathcal{C}_1 .
- The cluster-size moments $\mathcal{S}_m = \sum_C |C|^m$ with $m = 2, 4$, where the sum runs over all clusters C and $|C|$ denotes cluster size.
- An observable $\mathcal{S} := \max_C \max_{y \in C} d(x_C, y)$ used to determine the shortest-path exponent. Here $d(x, y)$ denotes the graph distance from vertex x to vertex y , and x_C is the vertex in cluster C with the smallest vertex label, according to some fixed (but arbitrary) vertex labeling.
- The indicators $\mathcal{R}^{(x)}$, $\mathcal{R}^{(y)}$, and $\mathcal{R}^{(z)}$, for the event that a cluster wraps around the lattice in the x , y , or z directions, respectively.

From these observables we calculated the following quantities:

- The mean size of the largest cluster $C_1 = \langle \mathcal{C}_1 \rangle$, which scales as $C_1 \sim L^{y_h}$ at p_c , with L the linear system size and $y_h = d - \beta/\nu$.
- The cluster density $\rho = \langle \mathcal{N}_c \rangle / V$, where $V = gL^3$ is the number of lattice sites, with $g = 1$ for the SC and DM lattices, $g = 2$ for the BCC lattice, and $g = 4$ for the FCC lattice.
- The dimensionless ratios

$$Q_1 = \frac{\langle \mathcal{C}_1^2 \rangle}{\langle \mathcal{C}_1 \rangle^2}, \quad Q_2 = \frac{\langle \mathcal{S}_2^2 \rangle}{\langle 3\mathcal{S}_2^2 - 2\mathcal{S}_4 \rangle}. \quad (1)$$

In the case of the Ising model, Q_2 is identical to the dimensionless ratio $Q_M = \langle M^2 \rangle^2 / \langle M^4 \rangle$, where M represents the magnetization.

- The mean shortest-path length $S = \langle S \rangle$, which at p_c scales like $S \sim L^{d_{\min}}$ with d_{\min} the shortest-path fractal dimension.

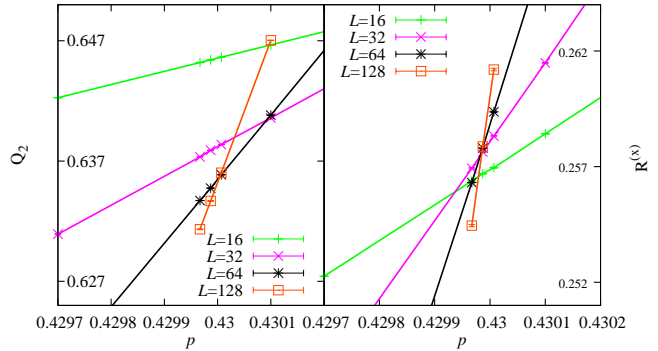


FIG. 2: Quantities Q_2 and $R^{(x)}$ as a function of p for the site percolation on the DM lattice with various sizes. In comparison with Q_2 , the plot of $R^{(x)}$ has a finer vertical scale, but still displays a clearer intersection. This suggests that $R^{(x)}$ suffers weaker finite-size corrections and provides a better estimator for p_c .

- The wrapping probabilities

$$\begin{aligned} R^{(x)} &= \langle \mathcal{R}^{(x)} \rangle = \langle \mathcal{R}^{(y)} \rangle = \langle \mathcal{R}^{(z)} \rangle, \\ R^{(a)} &= 1 - \langle (1 - \mathcal{R}^{(x)})(1 - \mathcal{R}^{(y)})(1 - \mathcal{R}^{(z)}) \rangle, \\ R^{(3)} &= \langle \mathcal{R}^{(x)} \mathcal{R}^{(y)} \mathcal{R}^{(z)} \rangle. \end{aligned} \quad (2)$$

Here $R^{(x)}$, $R^{(a)}$ and $R^{(3)}$ give the probability that a winding exists in the x direction, in at least one of the three possible directions, and simultaneously in the three directions, respectively. At p_c , these wrapping probabilities take non-zero universal values in the thermodynamic limit $L \rightarrow \infty$.

- The covariance of $\mathcal{R}^{(x)}$ and \mathcal{N}_b

$$g_{bR}^{(x)} = \langle \mathcal{R}^{(x)} \mathcal{N}_b \rangle - \langle \mathcal{R}^{(x)} \rangle \langle \mathcal{N}_b \rangle, \quad (3)$$

which scales as $g_{bR}^{(x)} \sim L^{y_t} = L^{1/\nu}$ at criticality p_c . Analogously, one defines $g_{sR}^{(x)}$ for site percolation, with \mathcal{N}_b being replaced with \mathcal{N}_s .

III. PERCOLATION THRESHOLD

The simulation on the SC lattice is up to linear size $L_{\max} = 512$, and the number of samples is about 5×10^8 for $L \leq 128$, 6×10^7 for $L = 256$, and 3×10^7 for $L = 512$. The Monte Carlo data and the analysis have been reported in Ref. [14]. For the other lattices, the simulation is less extensive with $L_{\max} = 128$. The number of samples is about 10^8 for lattice $L < 128$ and 4×10^7 for $L = 128$.

TABLE I: Percolation thresholds from the separate fits of the wrapping probabilities and the dimensionless ratios.

	Q_1	Q_2	$R^{(x)}$	$R^{(a)}$	$R^{(3)}$
DM ^b	0.389 591(2)	0.389 592(1)	0.389 589 2(5)	0.389 588 9(4)	0.389 590 0(5)
DM ^s	0.429 987(2)	0.429 985(1)	0.429 987 7(9)	0.429 987 5(6)	0.429 987 3(4)
SC ^b	0.248 811 96(6)	0.248 811 92(6)	0.248 811 85(3)	0.248 811 80(4)	0.248 811 81(9)
SC ^s	0.311 606 9(2)	0.311 607 1(2)	0.311 607 68(7)	0.311 607 74(6)	0.311 607 7(1)
BCC ^b	0.180 287 8(9)	0.180 288 3(6)	0.180 287 5(2)	0.180 287 4(2)	0.180 287 9(2)
BCC ^s	0.245 961 7(3)	0.245 961 5(2)	0.245 961 7(2)	0.245 961 70(11)	0.245 961 7(3)
FCC ^b	0.120 163 9(5)	0.120 163 3(3)	0.120 163 6(2)	0.120 163 6(2)	0.120 163 7(3)
FCC ^s	0.199 235 3(3)	0.199 235 2(2)	0.199 235 2(2)	0.199 235 14(11)	0.199 235 0(2)

TABLE II: Value of the amplitudes q_1 obtained from the separate fits of the wrapping probabilities and the dimensionless ratios.

	Q_1	Q_2	$R^{(x)}$	$R^{(a)}$	$R^{(3)}$
DM ^b	0.277(2)	0.642(3)	0.906(4)	1.236(5)	0.484(3)
DM ^s	0.193(2)	0.458(4)	0.652(3)	0.894(4)	0.341(3)
SC ^b	0.30(3)	0.90(7)	1.20(7)	1.80(9)	0.65(7)
SC ^s	0.22(2)	0.52(4)	0.70(4)	1.00(3)	0.36(3)
BCC ^b	0.644(3)	1.46(2)	2.084(8)	2.82(3)	1.12(2)
BCC ^s	0.30(1)	0.72(3)	1.04(2)	1.42(2)	0.56(1)
FCC ^b	1.19(9)	2.77(4)	3.91(3)	5.29(2)	2.08(2)
FCC ^s	0.449(3)	1.044(9)	1.507(5)	2.080(6)	0.794(4)

A. Separate fits

In numerical study of phase transitions, dimensionless ratios like Q_1 and Q_2 are known to provide powerful tools for locating critical points p_c . The wrapping probabilities have analogous finite-size scaling behaviors as the dimensionless ratios, and thus should also provide a useful method for estimating p_c . This is demonstrated in Fig. 2 for site percolation on the DM lattice. The intersections of the Q_2 data for different sizes L would approximately give the percolation threshold $p_c \approx 0.42995$, with uncertainty at the fourth or fifth decimal place. Due to their faster convergence as L increases, the intersections of the $R^{(x)}$ data would yield $p_c \approx 0.42999$. Similar phenomena are observed in all the percolation models studied in this work. Thus, it clearly suggests that the wrapping probabilities are more powerful tools for estimating p_c than the dimensionless ratios Q_1 and Q_2 .

According to the least-squares criterion, we fit Monte Carlo data for the quantities $R^{(x)}$, $R^{(a)}$, $R^{(3)}$, Q_1 and Q_2 separately for each percolation model to the following scaling ansatz

$$U(p, L) = U_0 + \sum_{k=1}^3 q_k (p - p_c)^k L^{ky_t} + b_1 L^{-1.2} + b_2 L^{-2}, \quad (4)$$

where y_t is the thermal exponent, U_0 is a universal

value depending on the quantity studied, and the q_k ($k = 1, 2, 3$) and b_j ($j = 1, 2$) are non-universal constants. A correction exponent of -1.2 is taken from the existing literature [14]. To evaluate the systematic errors caused by the scaling terms which are not included in the fitting ansatz, we set a lower cutoff $L \geq L_{\min}$ on the data and study the effect on the residual χ^2 as L_{\min} increases. Generally, we prefer the fit which produces $\chi^2/DF \sim O(1)$ (DF is the degree of freedom), and in which the subsequent increases of L_{\min} do not drop χ^2 by vastly more than one unit per degree of freedom. These principles apply in all the fits we carry out.

In the fits, we try different combinations of corrections to scaling: (1) both b_1 and b_2 are free to be determined by the data; (2), b_1 is set to 0 and b_2 is free; and (3), b_1 is free and b_2 is fixed at 0. We find that the correction amplitudes b_1 for the wrapping probabilities are rather small and in many cases are statistically consistent with zero. In contrast, for the dimensionless ratios one clearly observes a non-zero correction amplitude b_1 . Moreover, the amplitudes q_1 of the term $q_1(p - p_c)L^{y_t}$ in Eq. (4) for $R^{(x)}$ and $R^{(a)}$ are larger than those for Q_1 and Q_2 . This suggests that the wrapping probabilities are more sensitive to the deviation from criticality $p - p_c$ than the dimensionless ratios. These observations in the fits are reflected by Fig. 2.

Tables I and II summarize the percolation thresholds and the amplitudes q_1 from our preferred fits with combination (1), where the uncertainties are just the statistical errors. It can be seen that the estimates of p_c from different quantities are consistent with each other within the combined error margins. Further, the wrapping probabilities yield more accurate estimate of p_c than the dimensionless ratios by a factor of two or three.

B. Simultaneous fits

As described above, the Monte Carlo simulations for the SC lattice are much more extensive and are performed on larger system sizes than those on the other lattices. This leads to the more precise estimates of p_c and other parameters on the SC lattices. It is noted that for a given wrapping probability or dimensionless ratio,

TABLE III: Percolation thresholds and other non-universal parameters from the simultaneous fits of the wrapping probabilities. For all the fits, we set $L_{\min} = 32$ for $R^{(x)}$ and $R^{(3)}$ and $L_{\min} = 24$ for $R^{(a)}$, a , b_1 and b_2 are defined in Eq. (5).

M.	Obs.	p_c	a	b_1	b_2	M.	Obs.	p_c	a	b_1	b_2
DM ^b	$R^{(x)}$	0.389 589 22(18)	0.901(4)	0.012(13)	0.04(17)	DM ^s	$R^{(x)}$	0.429 986 96(19)	0.653(4)	0.023(9)	-0.53(11)
	$R^{(a)}$	0.389 589 1(1)	1.236(2)	-0.006(6)	0.08(7)		$R^{(a)}$	0.429 987 15(12)	0.895(2)	0.043(5)	-0.73(6)
	$R^{(3)}$	0.389 589 40(20)	0.480(1)	0.011(7)	0.1(1)		$R^{(3)}$	0.429 986 81(24)	0.3463(8)	-0.001(6)	-0.27(7)
SC ^b	$R^{(x)}$	0.248 811 84(3)	1.25(2)	0.001(5)	0.29(6)	SC ^s	$R^{(x)}$	0.311 607 65(5)	0.721(5)	0.024(4)	-0.44(5)
	$R^{(a)}$	0.248 811 85(3)	1.69(1)	-0.011(4)	0.78(4)		$R^{(a)}$	0.311 607 69(4)	0.992(4)	0.036(3)	0.02(3)
	$R^{(3)}$	0.248 811 94(5)	0.651(8)	0.004(4)	0.03(5)		$R^{(3)}$	0.311 607 70(8)	0.384(4)	0.002(4)	-0.46(4)
BCC ^b	$R^{(x)}$	0.180 287 6(1)	2.069(8)	-0.006(7)	0.2(1)	BCC ^s	$R^{(x)}$	0.245 961 48(6)	1.032(7)	0.020(4)	-0.41(5)
	$R^{(a)}$	0.180 287 57(9)	2.839(4)	-0.016(4)	0.01(5)		$R^{(a)}$	0.245 961 51(6)	1.407(3)	0.027(3)	-0.46(3)
	$R^{(3)}$	0.180 287 65(9)	1.102(3)	-0.004(4)	0.27(6)		$R^{(3)}$	0.245 961 46(9)	0.543(2)	0.001(3)	-0.19(4)
FCC ^b	$R^{(x)}$	0.120 163 79(7)	3.87(2)	0.004(8)	0.05(12)	FCC ^s	$R^{(x)}$	0.199 235 17(6)	1.48(3)	0.011(6)	-0.13(8)
	$R^{(a)}$	0.120 163 80(5)	5.311(6)	-0.008(4)	0.04(5)		$R^{(a)}$	0.199 235 22(5)	2.077(3)	0.018(4)	-0.13(4)
	$R^{(3)}$	0.120 163 72(18)	2.059(5)	0.014(6)	-0.1(1)		$R^{(3)}$	0.199 235 12(9)	0.804(2)	0.002(5)	0.09(6)

TABLE IV: Simultaneous fits of the wrapping probabilities $R^{(x)}$, $R^{(a)}$, $R^{(3)}$ for all models.

Obs.	y_t	U_0	U_2	U_3
$R^{(x)}$	1.1424(11)	0.257 80(6)	1.23(1)	-0.9(6)
$R^{(a)}$	1.1418(4)	0.460 02(2)	0.311(2)	-0.99(4)
$R^{(3)}$	1.1413(6)	0.080 46(4)	4.98(1)	9.7(4)

the value of U_0 in Eq. (4) is universal. To make use of the extensive simulation for the SC lattice, we carry out a simultaneous analysis of the Monte Carlo data for all the percolation systems studied in this work. More precisely, we choose the wrapping probabilities $R^{(x)}$, $R^{(a)}$, and $R^{(3)}$, and for each of them, the data is fitted by

$$U(p_j, L) = U_0 + \sum_{k=1}^3 U_k a_j^k (p_j - p_{c,j})^k L^{k y_t} + b_{1,j} L^{-1.2} + b_{2,j} L^{-2}, \quad (5)$$

where U_k ($k = 0, 1, 2, 3$) and y_t are universal; $j \in \{1, 2, \dots, 8\}$ refer to the site and bond percolation models on DM, SC, BCC and FCC lattice, and the parameters with subscript j are model-dependent. In other words, Eq. (5) can be regarded as a set of equations in which the universal parameters U_k and y_t are shared by all the percolation models. We expect that an accurate estimation of these universal parameters will be mainly achieved by the high-precision Monte Carlo data on the SC lattice, and as in return, this will help to improve the accuracy of p_c for the other models. Such a simultaneous analysis has been applied to the 3D Ising model, and the derivation of Eq. (5) can be found in Ref. [15].

The simultaneous fits by Eq. (5) follow the same procedure as that in the above subsection. We first note that among U_1 and a_j with $j = 1, \dots, 8$, there is one redundant parameter, and we thus set $U_1 = 1$.

Tables III and IV summarize the results for the uni-

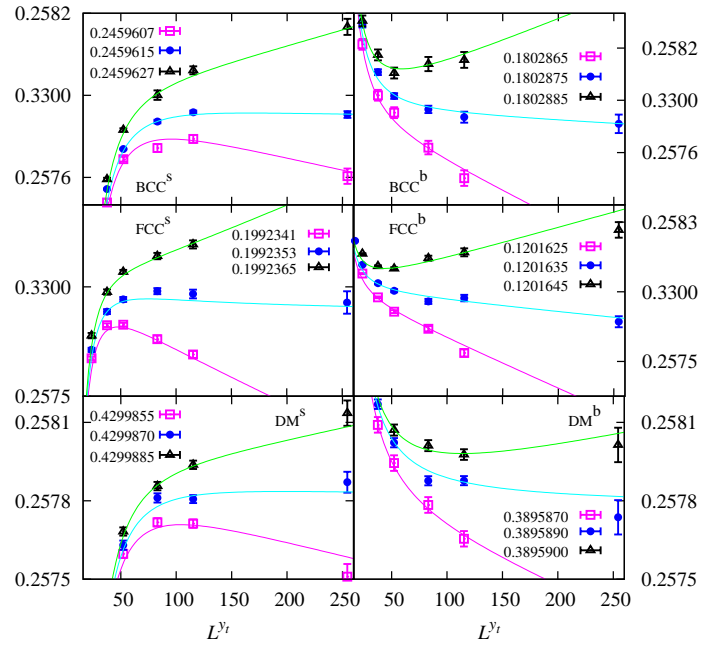


FIG. 3: $R^{(x)}(p, L)$ versus L^{y_t} at given p values which are in close to the estimated percolation thresholds for the site and bond percolation on the BCC (top), FCC (middle) and DM (bottom) respectively.

versal parameters, the percolation thresholds, and other non-universal constants, taken from the preferred fits with $L_{\min} = 24$ or 32 . In these fits, both the correction amplitudes $b_{1,j}$ and $b_{2,j}$ are left free. It can be seen from Tab. III that the leading correction amplitudes $b_{1,j}$ are rather small. In the cases that $b_{1,j}$ cannot be distinguished from zero within the statistical uncertainties, one can in principle exclude the leading correction term in the fits, which will further decrease the error margins.

In comparison with the results in Tab. I from the separate fits, the simultaneous analyses do significantly im-

TABLE V: Final estimates of percolation thresholds for the three-dimensional percolation models. The error bars include both statistical and systematic errors.

Lattice	Bond		Site	
	p_c (Present)	p_c (Previous)	p_c (Present)	p_c (Previous)
DM	0.389 589 2(5)	0.389 3(2) [17] 0.390(11) [19]	0.429 987 0(4)	0.430 1(4) [17] 0.426(+0.08,-0.02) [18]
SC	0.248 811 85(10)	0.248 811 82(10) [14] 0.248 812 6(5) [20]	0.311 607 68(15)	0.311 607 7(2) [14] 0.311 607 4(4) [16]
BCC	0.180 287 62(20)	0.180 287 5(10) [21]	0.245 961 5(2)	0.245 961 5(10) [20] 0.246 0(3) [22], 0.246 4(7) [23]
FCC	0.120 163 77(15)	0.120 163 5(10) [21]	0.199 235 17(20)	0.199 236 5(10) [20]

prove the estimates of p_c . By taking into account the results from different wrapping probabilities and from fits with different L_{\min} , we obtain the final estimates of p_c , as summarized in Tab. V. To check the reliability of the final quoted error margins in Tab. V, we plot the $R^{(x)}$ data at p_c and two other p values which are away from p_c about four or five times of final error bars. Precisely at $p = p_c$, the $R^{(x)}$ data should tend to a horizontal line as $L \rightarrow \infty$, whereas the data at $p \neq p_c$ will bend upward or downward. This is indeed clearly seen in these plots, some of which are shown in Fig. 3, confirming the reliability of our final results in Tab. V.

Also presented in Tab. V are existing estimates of p_c from the literature. It can be seen that this work does provide the percolation thresholds p_c with higher precision. For the bond and site percolation models on the DM lattices, such improvement is significant.

IV. RESULTS AT p_c

By fixing p at or very close to the estimated thresholds p_c in Tab. V, we study the covariances $g_{bR}^{(x)}$ and $g_{sR}^{(x)}$, the largest-cluster size C_1 , the shortest-path length S , and the cluster-number density ρ . From their finite-size-scaling behaviors, one can determine the thermal and magnetic renormalization exponent y_t and y_h , the shortest-path fractal dimension d_{\min} , and the universal excess cluster number b . In addition, we also obtain the thermodynamic cluster-number densities ρ_c for the studied percolation models.

A. Exponents y_t , y_h and d_{\min}

Following an analogous simultaneous analysis procedure, we fit the data of $g_{bR}^{(x)}$ and $g_{sR}^{(x)}$, C_1 , and S by the ansatz

$$\mathcal{A} = L^{y_A} (a_{0,j} + b_{1,j} L^{-1.2} + b_{2,j} L^{-2}), \quad (6)$$

where y_A is the universal scaling exponent. It is y_t for covariance $g_{bR}^{(x)}$ and $g_{sR}^{(x)}$, y_h for the largest-cluster size C_1 , and d_{\min} for the shortest-path length S . We obtain $y_t =$

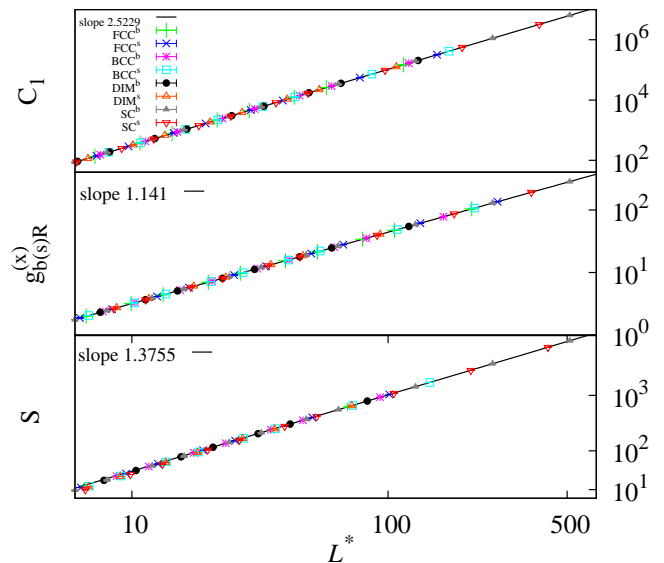


FIG. 4: Log-log plot of C_1 , $g_{b(s)R}^{(x)}$ and S versus the rescaled linear size L^* for all the 8 percolation models. We set $L = L^*$ for the bond percolation on the SC lattice, and rescale L by a constant factor (model-dependent) to collapse the numerical data.

1.141 3(15), $y_h = 2.522 93(10)$, and $d_{\min} = 1.375 5(3)$, which are consistent with the estimates in Ref. [14], with comparable or slightly better precision. For an illustration of these universal exponents, we plot in the log-log scale the data of these quantities versus the rescaled linear size $L^* = wL$, with constant $w = 1$ for the bond percolation on the SC lattice.

B. Excess number of clusters

The numerical data of the cluster-number density at percolation threshold for all the studied percolation models are simultaneously fitted by the scaling ansatz

$$\rho = \rho_c + V^{-1} (b + b_{1,j} L^{-2}), \quad (7)$$

TABLE VI: Simultaneous fits of ρ at the thresholds. Fitting parameter $L_{\min} = 16$ is set for all the models.

M.	ρ_c	b	b_1
DM ^b	0.231 953 78(4)	0.674 7(4)	-0.6(5)
DM ^s	0.075 519 45(2)		-1.1(4)
SC ^b	0.272 932 836(9)		1.1(2)
SC ^s	0.052 438 217(3)		-0.02(12)
BCC ^b	0.298 343 834(12)		0.3(3)
BCC ^s	0.040 045 144(3)		-0.76(9)
FCC ^b	0.307 691 25(2)		0.1(2)
FCC ^s	0.026 526 453(4)		-0.3(2)

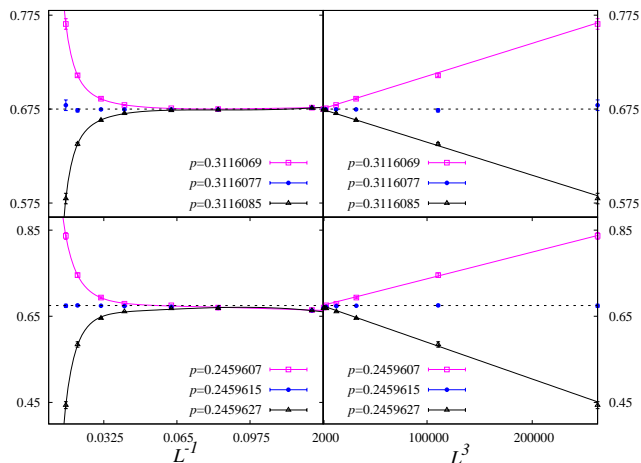


FIG. 5: Excess cluster number $V(\rho - \rho_c) (\equiv b)$ versus L^{-1} (left) and L^3 (right) for SC site (top) and BCC site (bottom) percolation models. The dashed straight lines represent constant 0.675.

where V is the number of lattice sites, and the correction amplitude b is known to be also universal and is referred to as the excess cluster number in Ref. [24]. The subleading correction is taken to be -2 . Due to the rapid decay of the correction term, the finite- L data of ρ quickly converges to the thermodynamic value ρ_c ; the well-determined values of ρ_c then aids in estimating the correction amplitude b from the small- L data. The fitting results of ρ_c and b are shown in Table VI. Taking into account some potential systematic errors—e.g., due to the small deviation of the simulated p value from p_c , we have the final estimate $b = 0.675(1)$.

An illustration of the excess cluster number b is shown in Fig. 5, where the values of $V(\rho - \rho_c)$ are plotted versus $1/L$ for the site percolation on the SC and the BCC lat-

tices. It can be seen that the $V(\rho - \rho_c)$ values at $p = p_c$ quickly converge to $b = 0.675$, while those for $p \neq p_c$ are either bending downward or upward. However, this does not imply that the cluster-number density ρ provides a good quantity for locating p_c . Near p_c , the finite-size behavior of $\rho(p, L)$ near threshold p_c can be described by

$$\rho(p, L) = \rho_c + f_1(p - p_c) + f_2(p - p_c)^2 + V^{-1}[b + h_1(p - p_c)L^{y_t} + h_2(p - p_c)^2L^{2y_t} + \dots], \quad (8)$$

where f_i and h_i ($i = 1, 2$) are non-universal parameters. The critical density ρ_c and the terms with f_i arise from the analytical part of $\rho(p, L)$ and do not depend on size L . They dominate the finite-size scaling of $\rho(p, L)$ but cannot be used to determine p_c . This is illustrated in Fig. 5. The critical singularity is reflected in the subleading terms with L -dependence. For the site percolation on the SC lattice, the fit yields $p_c = 0.311 604(2)$, with much larger error margin than those from wrapping probabilities.

V. SUMMARY

We present a Monte Carlo study of the bond and site percolation on several three-dimensional lattices, and obtain high-precision estimates of the percolation thresholds (Tab. V), the cluster density (Tab. VI), the wrapping probabilities (Tab. IV) and the excess cluster number $b = 0.675(1)$. These accurate scientific data can serve as a testing ground for future study of systems in the percolation universality class. More importantly, it is observed that the wrapping probabilities can be a useful and reliable approach for locating phase transitions. It is very plausible that this observation generally holds in other statistical-mechanical systems that have suitable graphical representations.

VI. ACKNOWLEDGMENTS

We thank R. M. Ziff and T. M. Garoni for helpful suggestions. This research was supported in part by NSFC under Grant No. 91024026, 11275185 and 11147013, and the Chinese Academy of Science. We also acknowledge the Specialized Research Fund for the Doctoral Program of Higher Education under Grant No. 20103402110053. The simulations were carried out on the NYU-ITS cluster, which is partly supported by NSF Grant No. PHY-0424082.

- [1] S. R. Broadbent and J. M. Hammersley, Proceedings of the Cambridge Philosophical Society **53**, 629 (1957).
 [2] D. Stauffer and A. Aharony, *Introduction To Percolation Theory* (Taylor & Francis, London, 1994), 2nd ed.

- [3] G. R. Grimmett, *Percolation* (Springer, Berlin, 1999), 2nd ed.
 [4] B. Bollobás and O. Riordan, *Percolation* (Cambridge University Press, 2006).

- [5] B. Nienhuis, in *Phase Transition and Critical Phenomena*, edited by C. Domb, M. Green, and J. L. Lebowitz (Academic Press, London, 1987), vol. 11.
- [6] J. L. Cardy, in *Phase Transition and Critical Phenomena*, edited by C. Domb, M. Green, and J. L. Lebowitz (Academic Press, London, 1987), vol. 11.
- [7] S. Smirnov and W. Werner, *Math. Res. Lett.* **8**, 729 (2001).
- [8] J. W. Essam, in *Phase Transition and Critical Phenomena*, edited by C. Domb and M. S. Green (Academic Press, New York, 1972), vol. 2.
- [9] X. Feng, Y. Deng and H. W. J. Blöte, *Phys. Rev. E* **78**, 031136 (2008), and references therein.
- [10] C. Ding, Z. Fu, W. Guo and F. Y. Wu, *Phys. Rev. E* **81**, 061111 (2010), and references therein.
- [11] G. Toulouse, *Nuovo Cimento Soc. Ital. Fis.* **B 23**, 234 (1974).
- [12] M. Aizenman and C. M. Newman, *J. Stat. Phys.* **36**, 107 (1984).
- [13] T. Hara and G. Slade, *Commun. Math. Phys.* **128**, 333 (1990).
- [14] J. Wang, Z. Zhou, W. Zhang, T. M. Garoni, and Y. Deng, *Phys. Rev. E* **87**, 052107 (2013).
- [15] Y. Deng and H. W. J. Blöte, *Phys. Rev. E* **68**, 036125 (2003).
- [16] Y. Deng and H. W. J. Blöte, *Phys. Rev. E* **72**, 016126 (2005).
- [17] S. C. van der Marck, *Int. J. Mod. Phys. C* **09**, 529 (1998).
- [18] A. Silverman and J. Adler, *Phys. Rev. B* **42**, 1369 (1990).
- [19] V. A. Vyssotsky, S. B. Gordon, H. L. Frisch, and
- [20] C. D. Lorenz and R. M. Ziff, *J. Phys. A* **31**, 8147 (1998).
- [21] C. D. Lorenz and R. M. Ziff, *Phys. Rev. E* **57**, 230 (1998).
- [22] R. M. Bradley, P. N. Strenski, and J. M. Debierre, *Phys. Rev. B* **44**, 76 (1991).
- [23] D. S. Gaunt and M. F. Sykes, *J. Phys. A* **16**, 783 (1983).
J. M. Hammersley, *Phys. Rev.* **123**, 1566 (1961).
- [24] R. M. Ziff, S. R. Finch, and V. S. Adamchik, *Phys. Rev. Lett.* **79**, 3447 (1997).